Lawrence Berkeley National Laboratory
Recent Work

Title
PHASE TRANSFORMATIONS IN NIOBIUM INVOLVING INTERSTITIALS

Permalink
https://escholarship.org/uc/item/38v0353r

Authors
Tome, L.I. Van
Thomas, G.

Publication Date
1963-10-01

University of California

Ernest O. Lawrence Radiation Laboratory

PHASE TRANSFORMATIONS IN NIOBIUM INVOLVING INTERSTITIALS

Berkeley, California

DISCLAIMER

UNIVERSITY OF CALIFORNIA

Lawrence Radiation Laboratory
Berkeley, California

PHASE TRANSFORMATIONS IN NIOBIUM INVOLVING INTERSTITIALS

L. I. van Torne and G. Thomas

October 1963

PHASE TRANSFORMATIONS IN NIOBIUM INVOLVING INTERSTITIALS

L. I. van Torne and G. Thomas

Inorganic Materials Research Division, Lawrence Radiation Laboratory
and Department of Mineral Technology, University of California
Berkeley, California

Abstract

A homogeneous phase transformation bcc Nb to a fcc lattice, probably NbO but containing C + N also, has been observed by transmission electron microscopy both in thin foils and in bulk specimens containing ~0.5 at. % interstitials after suitable aging treatments. The transformation proceeds in the following sequence: (a) ordering in Nb with interstitials taking $\frac{1}{2}\frac{1}{2}0$, $00\frac{1}{2}$ sites (b) formation of a precipitate in alternate prisms of Nb and NbO (c) growth to perfect NbO structure (d) recrystallization and possible disorder of NbO.

In thin foils the crystallographic features of the transformation are $[001]$Nb $||$ $[001]$NbO, (011)Nb $||$ (111)NbO. The habit planes are four variants of $\{101\}$ but only those inclined at less than 90° to the foil surface operate. In bulk specimens the habit planes are observed to be $\{021\}$ which is in accord with the crystallographic theory for martensitic transformations. The difference between bulk and thin film behavior is attributed to the lack of constraints in the later where the strains appear to be accommodated elastically. Conversely, in bulk specimens, dislocations are generated from the precipitate-matrix interfaces.

I. INTRODUCTION

During a recent investigation of the dislocation substructures formed in niobium[1] several hundred thin foils were prepared for transmission electron microscopy. Some of the thin foils were stored at room temperature for periods of up to 12 months. Special storage conditions were not necessary since the foils maintained their bright metallic luster over this period. Upon reexamination in the electron microscope these foils showed contrast effects, not observed previously, in the form of a cross-hatch pattern usually but not always along the thin edges. Examination of the diffraction patterns resulting from this structure showed that stage I of the transformation discussed below had begun to form. A search of the literature disclosed that a similar structure had been observed in thin foils of Ta[2] which was identified as ordering due to nitrogen.

A systematic investigation of the transformation in niobium thin foils was thus initiated. Some aged bulk specimens were also examined and the results obtained are discussed in this paper.

II. EXPERIMENTAL

Niobium sheets from the same stock as that used previously[1] were annealed at 2000°C for 1 hour and quenched in helium. The quench rate is estimated to be $\sim 10^3$°C/sec. Vacuum fusion and conductometric analysis of the material after this treatment showed the interstitial solute content to be.

$$(\text{at. \%}) \quad O = 0.42; \quad N = 0.11; \quad H = 0.48 \times 10^{-3}; \quad C < 0.78 \times 10^{-2} \, .$$

It should be noted that oxygen is the predominant impurity. Thin foils suitable for transmission electron microscopy were prepared from the annealed and quenched specimens by chemical polishing in a 60% conc. nitric acid-40% conc. hydrofluoric acid solution maintained at 0°C in an ice bath. Purer samples containing (in atomic percent) O = < 0.03, C = < 0.008, N = < 0.05, H = < 0.03, were also used but no transformation was ever observed in these samples.

The investigation of the transformation was conducted by three methods in a Siemens Elmiskop 1b electron microscope operated at 100kV. (1) The foils were pulse heated a number of times in the electron beam where the duration of the pulse was two seconds at a beam current of 40 μ amps.[*] Each pulse causes further transformation but there was no further change in structure between pulses. Thus, a thorough examination of the structures and corresponding diffraction patterns could be carried out at each stage of the transformation. (2) Freshly prepared foils were slowly brought up to the transformation temperature in the Siemens heating stage. The course of the transformation was recorded on ciné film taken at 10 frames per second. From this study the transformation was shown to occur isothermally in a matter of seconds at ~600°C. (3) In order to determine whether the transformation also occurred in bulk specimens, the annealed and quenched sheets were vacuum sealed in quartz tubes and aged at 670°C for 22 hours. Subsequent to this aging treatment thin foils were prepared as described above and then examined in the electron microscope.

---

[*] Pulse heating is accomplished simply by removing the condenser aperture.

III. RESULTS AND INTERPRETATION OF THIN FOIL EXPERIMENTS

1. The Transformation Product

Figures 1a - 1f show the changes in structure and diffraction patterns produced by pulse heating a foil originally in the [$\bar{1}$02] orientation, whilst Figs. 2-6 were all originally in <001> orientations. Figure 7 shows the transformation induced by isothermal aging of bulk specimens.

From these figures the general sequence of the transformation is as follows. (1) Formation of a cross-hatch pattern of contrast with the simultaneous appearance of many extra reflections in the diffraction patterns (Figs. 2, 3). (2) Nucleation, within the initially transforming area, of prisms which in thin foils are bounded by {110} planes. Internal striations are present within the prisms as they grow (Fig. 4). In bulk specimens the prisms are bounded by {021} (Fig. 7). (3) Growth of the prisms until they converge together with the elimination of the internal structure. The new phase is perfect fcc (Fig. 1). (4) Upon elevating the aging temperature to ~1000°C the new fcc phase recrystallizes with the appearance of fine structure on {111} normal to the surface (Figs. 5, 6).

It is convenient to consider Fig. 5 first, since this enabled the transformation product to be identified. The foil originally in the [100] orientation has transformed through stages similar to those shown in Figs. 2-5 and has recrystallized (Fig. 5a) giving rise to a diffraction pattern, Fig. 5b, which shows rings typical of those from a fcc lattice. It should be noticed that there is a preferred <110> texture in this ring pattern. Attempts at indexing the final single crystal diffraction patterns (e.g., Fig. 1f) based on niobium (bcc) or the known possible nitrides or carbides

of niobium corresponding to the compositions used here were unsuccessful except for NbC, NbN and NbO all of which have the NaCl structure. The average interplanar spacings calculated from measured reflection spacings on the diffraction patterns are shown in Table 1 together with the x-ray data reported for NbO, NbN and NbC. In view of the high oxygen content, and the results given in Table 1, it is concluded that the final transformation product is fcc NbO but probably containing other interstitial solutes in solid solution. Bearing this in mind it is convenient for the ensuing discussion to describe the transformation product as NbO.

From the hot stage experiments it was found that the transformation proceeded at an appreciable rate (such that all interstitials are consumed in less than 10 sec.) in thin foils at ~600°C(±10°). A calculation of the mean distance per sec. an oxygen atom can diffuse at this temperature gives a value of ~10μ. Hence, the transformation is not inhibited by the rate of diffusion of a component of the transformation product but proceeds until presumably all the available interstitials are consumed.

The transformation does not occur completely throughout the specimen, but only in isolated areas. Although the hot stage experiments enabled us to follow the transformation continuously, and to demonstrate its progress by means of ciné photography, for the purposes of investigating the details of the process it was much more convenient to allow the transformation to proceed step by step by pulse heating. Both methods gave identical results.

Table 1

Reflecting Plane	d-Spacings in A°			
	Average Measured	NbO[+]	NbN[(1)]	NbC[+]
111	2.58	2.43	2.55	2.58
200	2.22	2.10	2.20	2.23
220	1.55	1.49	1.56	1.58
311	1.33	1.27	1.33	1.35
222	1.29	1.21	1.27	1.29
400	1.10	1.06	1.10	1.12
331	1.01	0.969	1.01	1.03
420	0.982	0.943	0.985	0.999
a_0	4.43(calc.)	4.23[+]	4.41[*]	4.46[*]

+ ASTM card index. X-Ray Powder Data File.

* Crystal Structures, R. W. G. Wyckoff. Interscience, New York (1958).

(1) There is a Cubic→Hex. transformation reported for NbN[+], however, it probably precipitates in the cubic modification in Nb.

2. Crystallography of the Transformation

Figures 1a and 1b show a micrograph and diffraction pattern of a ($\bar{1}$02) area in niobium prior to pulse heating. It should be noticed that this area is nearly dislocation free. After 2 beam pulses the foil has transformed homogeneously to the structure shown in Fig. 1c. After four pulses the area shown in c has transformed completely by growth of the transformation prisms (Fig. 1c) and the new orientation is shown in Fig. 1f. The foil is now in the ($\bar{1}$12)NbO orientation. The orientation relationship in this case is thus ($\bar{1}$02)Nb||($\bar{1}$12)NbO. Experiments on a (100)Nb foil showed that the orientation change was (100)Nb → ($\bar{1}$10)NbO (e.g., Figs. 5b, 6b). These results characterize a simple bcc → fcc transformation in which planes [hkℓ] of niobium transform to planes {HKL} of NbO where H = (h+k), K = (k-h), and L = ℓ. This shows that the "new" lattice is related to the "old" lattice by a 45° rotation about the common z-axis, i.e., [001]. Thus the new $\underline{a}$' axes are given by $\underline{a}$ [1$\bar{1}$0] and $\underline{a}$ [1$\bar{1}$0] respect to niobium.

The orientation relationships are shown by the (001) stereographic projection in Fig. 8. Planes (001)Nb (111)Nb (121)Nb, etc., become (111)NbO (201)NbO (311)NbO, etc., by an expansion along [001]Nb. The angular shift required to bring these planes into concidence (~10°) corresponds to an expansion along [001] of 1.13 Å. Insertion of interstitial atoms in the $00\frac{1}{2}$ sites effectively produces such an expansion.[*] There is a corresponding contraction of ~10% along [100] and [010]Nb due to interstitials at $\frac{1}{2}\frac{1}{2}0$ sites, as the complete NaCl structure of the new phase is attained. From the data in Table 1, and with a_0 for Nb = 3.3 Å the principal strains are

---

[*] On a hard sphere model an oxygen atom at $00\frac{1}{2}$ produces an expansion = 1.32 Å, whereas a nitrogen atom produces an expansion = 1.4 Å. The observed change from diffraction patterns (Table 1) is 1.13 Å.

calculated to be 1.34 and 0.942. The net result is simply the insertion of sheets of interstitial atoms between the (101)(011)($\bar{1}$01) and (0$\bar{1}$1) close packed planes in niobium, so producing alternate {111} sheets of Nb and interstitial atoms in the new lattice. The structural relationships are shown in Fig. 9. The first stage of the transformation is thus expected to be one of ordering of interstitials between the four ⟨101⟩ habit planes in Nb.

3. Stages in the Transformation

The pulse heating and hot stage experiments have shown that two principal stages occur during the transformation. The first stage corresponds to the formation of a cross-hatch pattern of contrast parallel to [$\bar{1}$10] and [110] traces in [001] foils which usually, but not always, originates at the foil edges and progress inwards (Figs. 2b and 3a). Simultaneously faint extra reflections appear in the corresponding diffraction patterns (compare Figs. 2a and 2c). In the ⟨001⟩ orientations, the initial extra reflections appear as four satellites around the principal reflections. By examination of other orientations it was found that these satellites correspond to intersection of [101], [011], [$\bar{1}$01], [0$\bar{1}$1], rel-rods with the cube planes of the reciprocal lattice (Fig. 10). This indicates disturbances in the spacing of these planes as expected if interstitial atoms are diffusing to the $00\frac{1}{2}$ and $\frac{1}{2}\frac{1}{2}0$ sites. The dark field image of the 1$\bar{1}$0 reflection and its satellites is shown in Fig. 3c. Reversal of contrast in the cross-hatch pattern occurs. It is concluded that this form of contrast is due to elastic strains associated with order and not from alternately ordered-disordered regions. This conclusion is

supported by the fact that extinction contours (i.e., primary reflecting planes) are strongly kinked indicating that local elastic strains occur at the foil surfaces and by the fact that the striations can be made to grow and shrink during observation (see Fig. 3a and 4a). This is most clearly demonstrated by cine-photography.

In the [001] orientation (Fig. 3) the maximum strain due to ordering is normal to the four {101} planes at 45° to the foil surface with a resolved shear component $\vec{R}$ acting parallel to the plane of the foil surface and the resolved shear component $\vec{S}$ acting normal to the plane of the foil. It is only the former component which can give rise to strain contrast since $\vec{g} \cdot \vec{S} = 0$ where $\vec{g}$ is the reciprocal lattice vector for a particular reflecting plane. As shown in Figs. 8 and 11, the habit planes for the transformation are the four variants $(101)(011)(\bar{1}01)$ and $(0\bar{1}1)$. Now the cross hatch contrast makes traces along [110] and [$\bar{1}$10] which are the net traces of (101) $(011)(\bar{1}01)$ and $(0\bar{1}1)$ intersections (Fig. 11). They cannot be traces of (110) or ($\bar{1}$10) but they could be traces of $(112)(\bar{1}12)(\bar{1}\bar{1}2)$ and $(1\bar{1}2)$. These are planes upon which the maximum resolved shear strain acts. Furthermore, the shears are of opposite sign for planes at 90° to each other and will eventually cancel at short distances. The alternation in contrast along a given trace can thus be understood in terms of reversal of the sign of the strain. At an extinction contour $\bar{g}$ is the same sign but $\vec{g} \cdot \vec{R}$ changes from positive to negative everywhere that R changes sign. In other words the contour will be kinked in alternate directions. This effect is observed in Figs. 3a and 4a. However, much of the kinking is also due to the $\bar{S}$ shears within the foil which cause surface eruptions. Thus the contrast observed is consistent with the interpretation given, and is similar to

that observed for order-induced strains, in e.g., Cu-Be[3] and Cu-Au[4,5].
It should be noted, however, that in the case considered here superlattice
reflections are not resolved in the diffraction patterns.

The second stage in the transformation corresponds to the appearance
of small prisms bounded by the habit planes, e.g., in Figs. 1c, 3, and 4.
In the <100> orientations four sided prisms are formed as illustrated by
Fig. 12. In the earliest stages the diffraction patterns are very complex
as shown by Fig. 2c. However, all these spots can be satisfactorily
accounted for by the reciprocal lattice shown in Fig. 10a and including
<112> and <201> rel-rods. The <112> distortions in <001> orientations
are expected in view of the fact that these planes suffer the maximum
resolved shear strains due to ordering as discussed above. A possible
explanation of <201> rel-rods will be given later (Section 5). The
constructed [001] diffraction pattern is shown in Fig. 10b which agrees
very well with the observed pattern in Fig. 1c. The effect of ordering of
interstitials between the {101} habit planes is to produce localized Nb → NbO
transformation, partially or totally, depending on the interstitial
concentration. Such changes distort the reciprocal lattice from the ideal
point lattice for a perfect crystal.[6] Further, the shape factor of
regions of the crystal which are bounded by the precipitate causes a streaked
reciprocal lattice.[7] Thus, these effects can account for the observed
diffraction effects.

An interesting feature of the transformation is the alternating dark
and light ribbons of contrast within the prisms (e.g., Figs. 1c, 4c and 4d).
These make traces corresponding to {110} planes inclined to the foil surfaces.

Figure 12 is a sketch of the transforming regions. When this Figure is compared to Fig. 4b, it can be seen that each prism is divided into blocks corresponding to the traces of intersections of two sets of habit planes within the prism defined by the other two sets as shown in Fig. 11. The contrast can be reversed by tilting or in dark field images. These traces have disappeared after final growth of the prisms has occurred (Fig. 1e).

This contrast is persistent only during the growth stages of the prisms (e.g., Figs. 1c, 4c and d) when the structure, as deduced from the diffraction patterns (e.g., Fig. 1d), is still essentially bcc, i.e., the transformation is still very incomplete. When transformation is completed, Fig. 1e, this contrast has disappeared and the diffraction patterns are those of a normal fcc structure (Fig. 1f). Although the contrast is similar in appearance to that observed in transformed Cu-Al[8] (faulting) and CuAu II[5] (twinning), the observations given above suggest that the contrast in this case is due to partial transformation to NbO within each prism. Since each block transforming to NbO undergoes ~30% expansion along [001] the adjacent regions suffer shear strains in a direction parallel to the surface (which will result in contrast) and shear strains normal to the surface which give rise to surface tilts. The latter causes kinking of extinction contours. In the [001] foils where all four habit planes operate the contrast appears complicated due to overlapping (e.g., Fig. 4d). This effect is more clearly seen in the sketches of Fig. 12. In these cases the net traces are those corresponding to the intersections of the operating habit planes (Fig. 11). Similar arguments explain the contrast observed in the other orientations examined (e.g., Fig. 1c).

The structure within a transforming prism can be regarded as faulted, since the atoms on (110)Nb planes are arranged as follows:

Transformed	Untransformed	Transformed

Nb - O - Nb - Nb - Nb - Nb - Nb - Nb - O - Nb - O - Nb
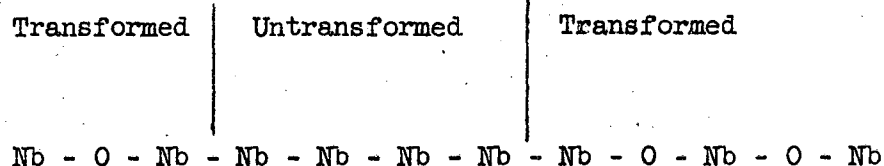
In other words the striations within the prisms represent ordered and non-ordered regions. If the striations were due to twinning in the transformation product, appreciable fcc and twin related reflections would be expected in the diffraction patterns. A comparison of Figs. 1d and 1f shows that this is not the case. Furthermore twins would be expected to persist after final growth, yet as shown in Figs. 1e and f, no striations nor twin spots are observed. Finally it should be noted that the striations cannot be slip markings in NbO because the traces do not correspond to {110}NbO which are the expected slip planes in the NaCl structure[9]. The division of the crystal into blocks bounded by {110} accounts for the persistence of <101> streaks observed in the diffraction patterns of Figs. 1-4. As the prisms grow and untransformed blocks within them transform to NbO the material within prisms becomes more perfect and <112> <201> and <110> rel-rods corresponding to the changing Nb lattice disappear. In the final stage relatively perfect single crystals of NbO are obtained.

4. Recrystallization of NbO

The structure shown in Fig. 1e can be made to recrystallize by heating to 1000°C and higher. Discreet nuclei of new grains are observed to form

(Fig. 5a), not entirely randomly but as shown by Fig. 5b they tend to retain the texture of the original orientation ([1$\bar{1}$0]NbO in the case of Fig. 5a). As these regions grow they merge into each other producing large single crystals differing only slightly in orientation by forming small angle dislocation boundaries (Fig. 5c, 6a). Within each new crystal, narrow bands parallel to {111} traces are observed. However, these traces always correspond to {111} planes normal to the foil surface and only one of the {111} planes are involved in any single grain (Fig. 6a). The diffraction patterns are now streaked again but along <111> NbO as seen in Fig. 6b. Since the density of the striations in the micrographs is low and as they are very narrow, no shifts in diffraction spots are observed neither are there any intensity peaks along the streaks between principal reflections. It is not possible therefore to decide whether or not this effect is due to growth faults or twinning but their appearance is rather typical of annealing twins. Although faulting is not expected in the NaCl structure since nearest like neighbors would be produced, it is possible that faults of the type Nb-0 Nb - Nb - 0 can be formed in NbO without much energy expenditure due to the screening effect of the electron shells in Nb. Such a structure must exist at interfaces if the striations are twins.

The mechanism of recrystallization is not the same as that in deformed and annealed materials[10] e.g., no dislocations are observed. However, it can be seen that (111) striations appear in the areas which are about to recrystallize (Fig. 6a) and that new grains generally grow parallel to these (111) planes. This suggests that the observed effects may be associated with disordering of the NbO lattice but the fcc structure is still maintained.

IV. TRANSFORMATION IN BULK SPECIMENS

In order to determine whether or not the transformation just described is solely a phenomenon occuring in thin foils, bulk specimens of Nb of the same composition as those used in the thin foil experiments were aged for 22 hours at 670°C. Figure 7 shows typical microstructures obtained of the bulk impure material (~0.5 at. % interstitials). Transformation has occurred in which tapered prisms of NbO form. The orientations are (112) in Fig. 7a and (153) in Fig. 7b. Trace analyses showed unambiguously that the interfaces Nb/NbO are {201} planes and not {110} as observed in thin foils. The broad striped contrast at A is rather faint and is very sensitive to orientation, suggesting that as in foils, it represents strain contrast associated with ordering. There is a possibility that these regions may be ordered domains but again no superlattice reflections have been detected. It can also be seen that considerable dislocation generation has occurred from the precipitate-matrix interface. These are observed in areas where the transformation product has formed (notice their absence in regions A of Fig. 7), i.e., when the elastic strains reach a maximum. Thus unlike the thin foil results where no dislocations were observed, the strains due to transformation in bulk material are relieved by plastic deformation. This suggests that although the transition is diffusion controlled it may proceed martensitically, (see Section 6). More experiments are being done on bulk materials to investigate the transformation mechanism in more detail.

V. COMPARISON OF BULK AND FOIL BEHAVIOR

From the diffraction data obtained in Table 1 the principal strains involved in the transformation were calculated to be 1.34 and 0.942. These

correspond to a simple (reverse) Bain strain and suggests that the reaction although diffusion controlled could have the crystallographic features of a martensitic reaction.

Weschler, Lieberman and Read[11] have shown that the habit plane of a shear transformation can be predicted when the original and final structures and their respective lattice parameters are known. The application of this theory to the Nb-NbO transformation predicts that the direction cosines of the habit plane are, e.g., -0.070, 0.1914, 0.1414. The miller indices of the predicted plane are {7, 90, 41}. This irrational plane is 5°7' away from (021) - the latter being the observed habit plane in bulk specimens but not in thin foils. In order to distinguish between {021} and {101} habit planes, foil orientations are required which do not give coincident traces for these two sets of planes. A distinction cannot be made with an [001] foil. However, trace analysis on ($\bar{1}$02) and (111) foils show decisively that the habit plane is {101} when the transformation occurs in foils. Furthermore, the observed operative {101} planes are those which are inclined to the thin foil surface at less than 90°. For example, in Fig. 13 only three {101} planes operate. This is to be expected since these are the planes upon which the strains induced by the transformation are most easily accommodated by elastic buckling of the foil, i.e., the material transforms to take advantage of the lack of constraints in the direction of the foil thickness.

The {021} habit plane observed when the transformation occurs in the bulk is in agreement with that predicted by the WLR theory. The existence of a habit plane in thin foils which differs from that predicted by the theory arises from the approximation to a two dimensional body in thin foils, i.e., there is an additional degree of freedom in the latter case.

In bulk specimens the transformation strains are accommodated by plastic deformation.

There is, however, some tendency for {021} habit planes to operate in the foils in the earliest stages. This is evident by the appearance of reflections in the diffraction patterns due to intersection of the Ewald Reflecting sphere with {021} rel-rods in stage I (e.g., Figs. 2c, 10b). Now as the strains build up and are relieved by elastic buckling during the transformation, {101} habit is then assumed so that simple relationships are then obeyed. Pitsch[12] has also observed simple crystallographic orientations in martensitic reactions in thin foils of iron alloys but not in bulk material.

VI. ORIGIN OF THE TRANSFORMATION

In order for the transformation to occur during aging to NbO or NbN or NbC or mixtures of all three, the local concentration of interstitials must be very high indeed. The question arises whether or not in thin foils the reaction is due to contamination, e.g., during heating in the electron microscope. The most likely source is carbon due to decomposition of hydrocarbon in the impure vacuum. However, in the purest foils examined (see Section 2) no transformation was ever observed even after heating for long times above 600°C. Since the transformation occurs in inpure bulk Nb it is concluded that the interstitials involved must be those orginally present in the material. However, there is undoubtedly some pick-up of carbon during aging in the microscope and possibly oxygen pick-up during chemical polishing in the preparation of thin foils.

VII. CONCLUSIONS

In niobium containing ~0.5 at. % interstitials a homogeneous phase
transformation to a fcc lattice occurs during annealing in local regions.
This transformation initiates by diffusion of interstitials until the local
concentration is high enough to produce appreciable order between {101}
planes in niobium. In thin foils the precipitate forms as prisms
bounded by those of the four (101), (011)($\bar{1}$01)(0$\bar{1}$1) habit planes dictated
by the orientation of the sample. The orientation relationships are
[10l]Nb || [001]fcc, (011)Nb || (111)fcc. These crystallographic changes are
produced by interstitial atoms diffusing to (00$\frac{1}{2}$)($\frac{1}{2}\frac{1}{2}$0) sites with an
expansion of ~30% along [001]Nb and a contraction of ~10% along [100]
and [010]. The resultant structure is that of NaCl. Heating to ~1000°C
results in recrystallization which may be a disordering reaction with the
formation of twins or growth faults. The habit planes observed in bulk
specimens are {201} as predicted by the crystallographic theory for
martensite reactions. The difference in behavior between thin foils and
bulk specimens is attributed to be essentially two dimensional character
of the former. Finally, in view of these results, it may be remarked that
the usual recovery and annealing treatments given to impure Nb may produce
transformations (locally) of the type described here. The same is probably
true for other bcc metals, e.g., Ta[2]. In this event, the possible effects
of the resulting substructures upon the properties of the material must be
taken into account.

Acknowledgement

References

1. L. I. van Torne and G. Thomas, Acta Met., 11, 881 (1963).

2. D. P. Seraphim, N. R. Stemple, D. T. Novick, J.A.P., 33, 136 (1962).

3. W. K. Armitage, P. M. Kelly and J. Nutting, Fifth Internatl. Cong. for Electron Microscopy, Philadelphia (1962), Interscience, N. Y., p. K4.

4. M. Hirabayashi and S. Weissmann, Acta Met., 10, 25 (1962).

5. A. M. Hunt and D. W. Pashley, J. Austr. Inst. Metals, 8, 61 (1963).

6. R. D. Burbank and R. D. Heidenreich, Phil. Mag., 5, 373 (1960).

7. R. Hosemann and S. N. Bagchi, Direct Analysis of Diffraction by Matter, 96ff. North Holland Pub. Co. - Amsterdam (1962).

8. H. Warlimont and P. R. Swann, Acta Met., 11, 511 (1963).

9. E. Schmid and W. Boas, Kristallplastizität, p. 239, Springer, Berlin, (1935) and English trans., Hughes, London, (1950).

10. J. E. Bailey and P. B. Hirsch, Proc. Roy. Soc., A 267, 11 (1962).

11. M. S. Wechsler, D. S. Lieberman and T. A. Read, Trans. AIME, 197, 1503 (1953).

12. W. Pitsch, Phil. Mag., 4, 577 (1959).

Figure Captions

Fig. 1. (a) [$\bar{1}$02]Nb foil in initial state.

(b) Diffraction pattern of (a).

(c) The same field of view as (a) after two beam pulses; 40 μ amps at one sec/pulse.

(d) Diffraction pattern of (c). Note intensity spikes on (21$\bar{1}$) and ($\bar{2}$1$\bar{1}$) reflections due to transformation on the habit planes (0$\bar{1}$1) and (011).

(e) The same field of view as (a) after six beam pulses.

(f) Diffraction pattern of (e). FCC crystal in [$\bar{1}$12] orientation.

Fig. 2. (a) Diffraction pattern of an [011]Nb crystal in the initial state.

(b) The same area after one beam pulse. Note cross-hatch pattern at A due to strain contrast and formation of prism due to intersecting {011} habit planes at B.

(c) Diffraction pattern from region A in (b). Compare this diffraction pattern to that which is constructed in Fig. 10b.

Fig. 3. (a) A magnification of a region similar to A in Fig. 2(b). Note kinking of the extinction contour due to elastic buckling of the foil on the left of the Figure.

(b) Diffraction pattern of (a). Asymmetry of the pattern is due to elastic buckling of the foil.

(c) Dark field image of (a) formed from (1$\bar{1}$0) and satellites.

Fig. 4. (a) [001]Nb crystal after two beam pulses. Note kinking of extinction contours due to elastic buckling of the foil.

(b) Diffraction pattern of (a). Intensity spikes on the primary reflections are due to transformations on the habit planes ($\bar{1}$01), (0$\bar{1}$1), (011) and (101).

(c) Same field of view as (b) after three beam pulses.

(d) A magnified view of the prisms formed by the four operating habit planes. Compare area A with Fig. 12.

(e) Diffraction pattern in region where prisms have formed. Note that the intensity spikes due to the {011} habit planes persist whereas the other extra reflections of Fig. 2c have disappeared.

Fig. 5. (a) Recrystallization of the transformation product at ~1000°C in the heating stage. Note the preferred orientation of the nuclei.

(b) Diffraction pattern of (a): the sequence of the diffraction rings correspond to FCC structure. Original foil in [100], notice preferred <110> texture in ring pattern.

(c) Further growth of the crystals in (a).

Fig. 6. (a) The same area as Fig. 5, at a more advanced stage of crystal growth. Note the traces of (111) planes that are perpendicular to the foil surface.

(b) [1$\bar{1}$0] FCC diffraction pattern from the large crystals at the top of Fig. 6a showing intensity spikes in [$\bar{1}\bar{1}$1] and [111].

Fig. 7. (a) [112]Nb crystal showing the morphology of the transformation which occurs in the bulk after twenty-two hours aging at 670°C. In the bulk specimen the habit planes are near {021}.

(b) As (a) but foil orientation [15$\bar{3}$].

Fig. 8. A composite [001] sterographic projection of Nb and NbO crystals showing the relative position of poles in Nb and NbO after transformation in thin foils.

Fig. 9. A sketch showing the crystallographic relationship between Nb and NbO after transformation in thin foils.

Fig. 10. (a) Four unit cells of the Nb reciprocal lattice showing rel-rods due to shape factor of (011), (0$\bar{1}$1), (101) and ($\bar{1}$01) planes. The {112} and {021} intensity spikes have been omitted for clarity.

(b) Intersection of the Ewald Reflecting Sphere with the (001) plane of the Reciprocal Lattice.

Fig. 10 continued:

key: ⊘ Primary reflections.

◻ (101), (011), (0Ī1) and (Ī01) intensity spike intersections.

△ (201), (102), (Ī01), (Ī02), (021), (012), (0Ī1) and (0Ī2) intensity spike intersections.

• (1Ī1), (121), (Ī21), (Ī21), (Ī21), (2Ī1), (ĪĪ1), (Ī11) and (211) intensity spike intersections.

Fig. 11. The [001]Nb sterographic projection showing the four operative habit planes (101), (011), (Ī01) and (0Ī1) in a foil and the traces of their intersections.

Fig. 12. A sketch showing how the contrast of Fig. 4d can arise from intersections and overlap of the four operating habit planes.

Fig. 13. Transformation in [111]Nb foil (a) notice that only the three {110} habit planes at 35° to the foil surface operate, (b) diffraction pattern showing three {101} rel-rods corresponding to the operating habit planes.
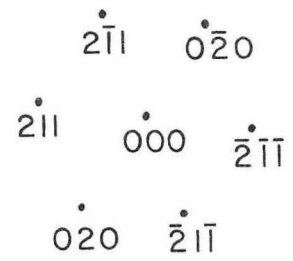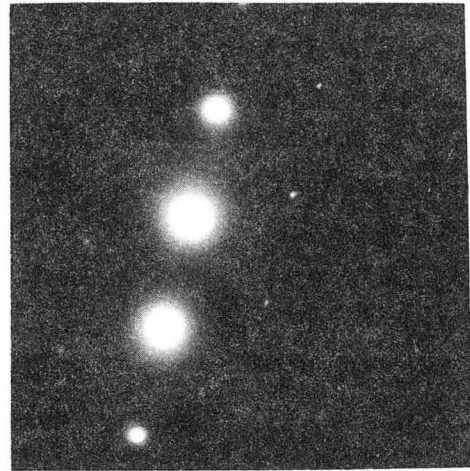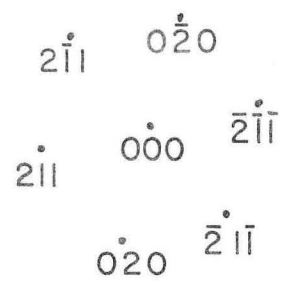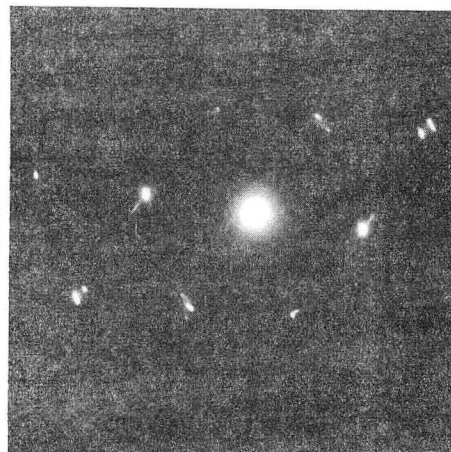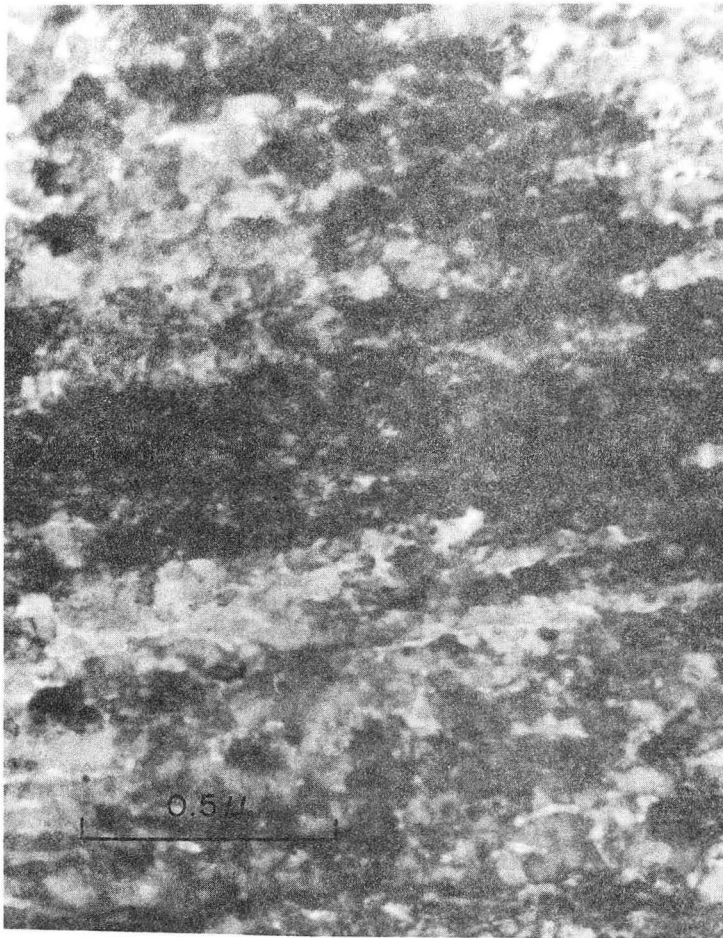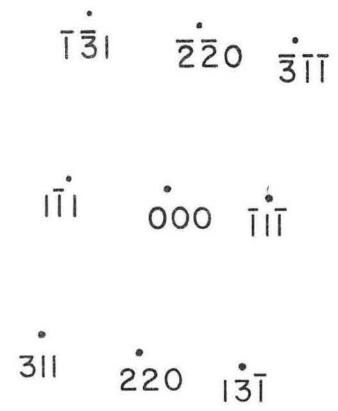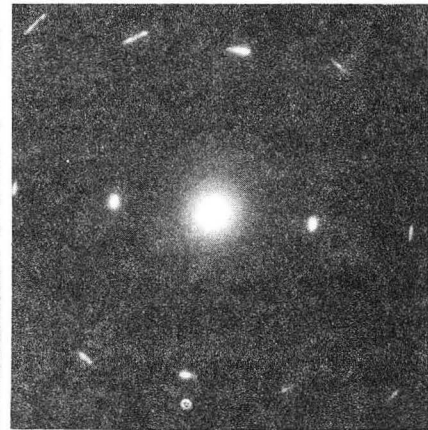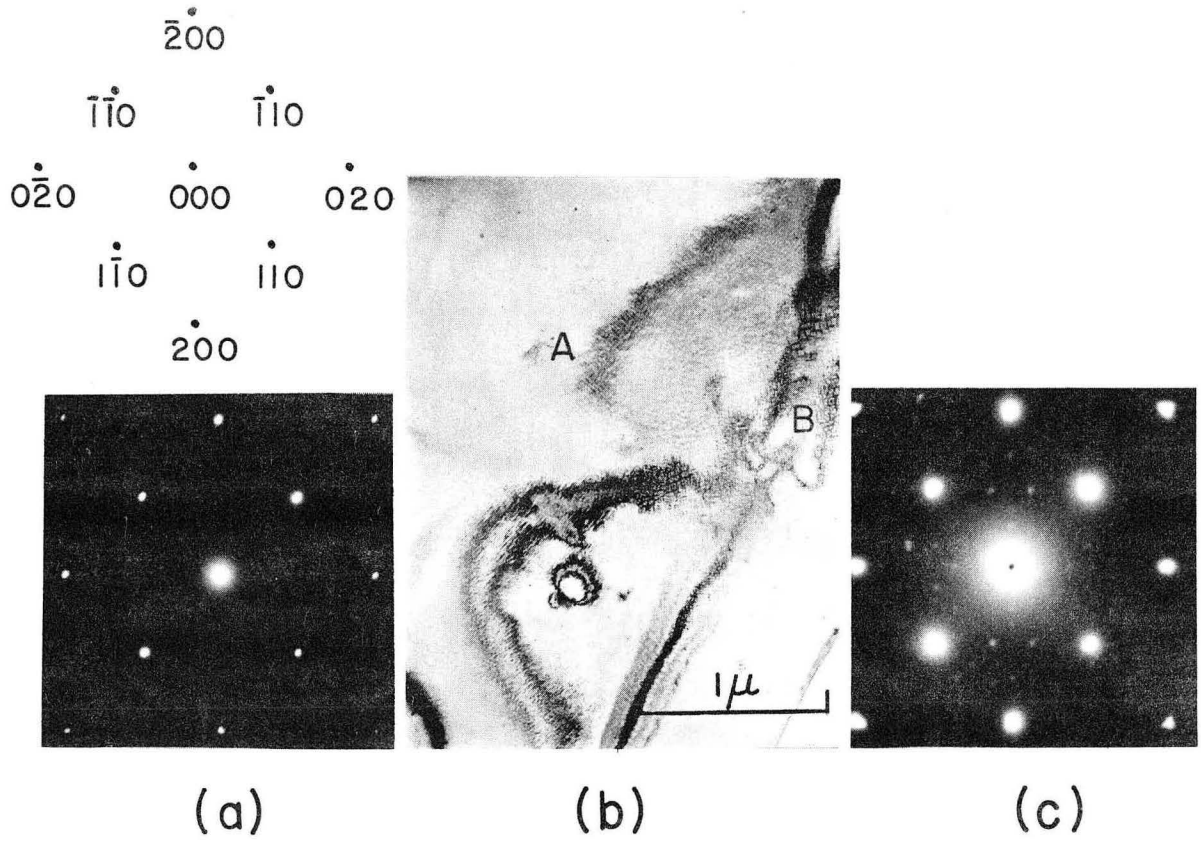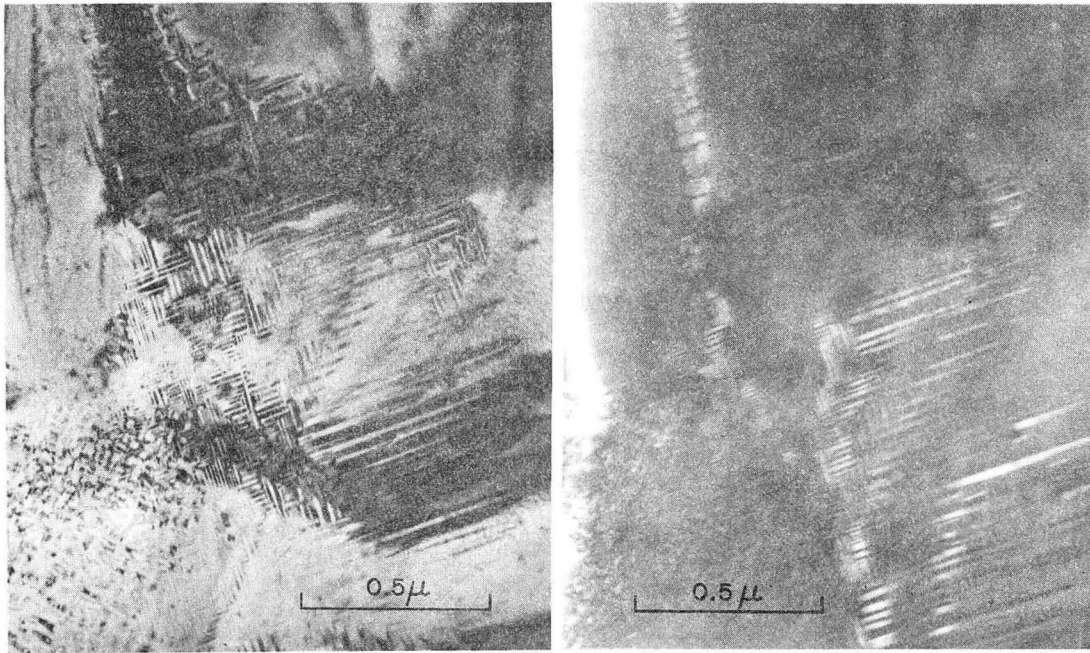
2̇1̄1   0̇2̄0

2̇11   0̇00   2̄̇1̄1̄

0̇2̇0   2̄̇11̄

(a)   (b)

ZN-3945

Fig. 1. (a,b)

(c)

(d)

$2\overset{.}{1}1$ $0\overset{.}{2}0$

$2\overset{.}{1}1$ $0\overset{.}{0}0$ $\overline{2}\overset{.}{1}\overline{1}$

$0\overset{.}{2}0$ $\overline{2}\overset{.}{1}\overline{1}$

ZN-3944

Fig. 1. (c,d)

$\bar{1}\bar{3}1$　$\bar{2}\bar{2}0$　$\bar{3}\bar{1}\bar{1}$

$1\bar{1}1$　000　$\bar{1}1\bar{1}$

$3\bar{1}1$　220　$13\bar{1}$

(e)　(f)

ZN-3951

Fig. 1. (e, f)

$\bar{2}00$

$\bar{1}\bar{1}0$ $\bar{1}10$

$0\bar{2}0$ 000 020

$1\bar{1}0$ 110

200

(a)   (b)   (c)

ZN-3943

Fig. 2.

(a)

(c)

$\bar{1}\bar{1}0$ $\bar{2}00$

$\bar{1}10$

$1\bar{1}0$ 000

$\bar{2}00$ 110

(b)

ZN-3952

Fig. 3.

(a)   (b)

$\overset{\bullet}{\bar{2}}00$

$\bar{1}\overset{\bullet}{\bar{1}}0$ $\bar{1}\overset{\bullet}{1}0$

$0\overset{\bullet}{\bar{2}}0$ $0\overset{\bullet}{0}0$ $0\overset{\bullet}{2}0$

$1\overset{\bullet}{\bar{1}}0$ $1\overset{\bullet}{1}0$

$\overset{\bullet}{2}00$

ZN-3942

Fig. 4. (a,b)

$\overline{2}00$

$\overline{1}\overline{1}0$ $\overline{1}10$

$0\overline{2}0$ 000 020

$1\overline{1}0$ 110

200

(c)   (d)   (e)

ZN-3947

Fig. 4 (c, d, e)

(b)

(c)

(a)

ZN-3948

Fig. 5.

(a)

$0\dot{0}2$ $\dot{1}\dot{1}1$

$\bar{1}\bar{1}\dot{1}$ $0\dot{0}0$ $1\dot{1}\bar{1}$

$\bar{1}\dot{1}\bar{1}$ $0\dot{0}\bar{2}$

(b)

0.5 μ

Fig. 6.

ZN-3950

(a)

(b)

ZN-3946

Fig. 7.

Fig. 8.
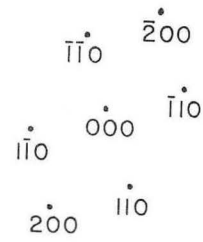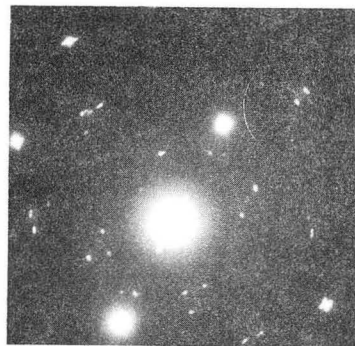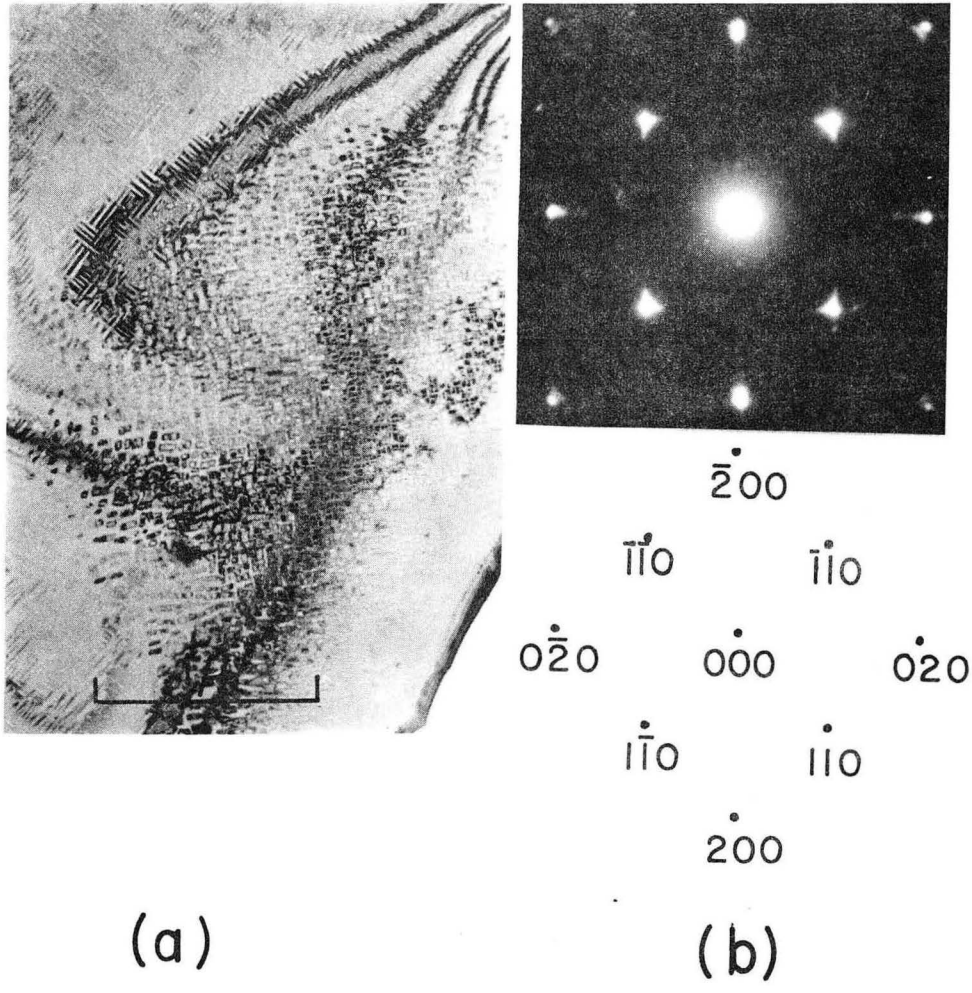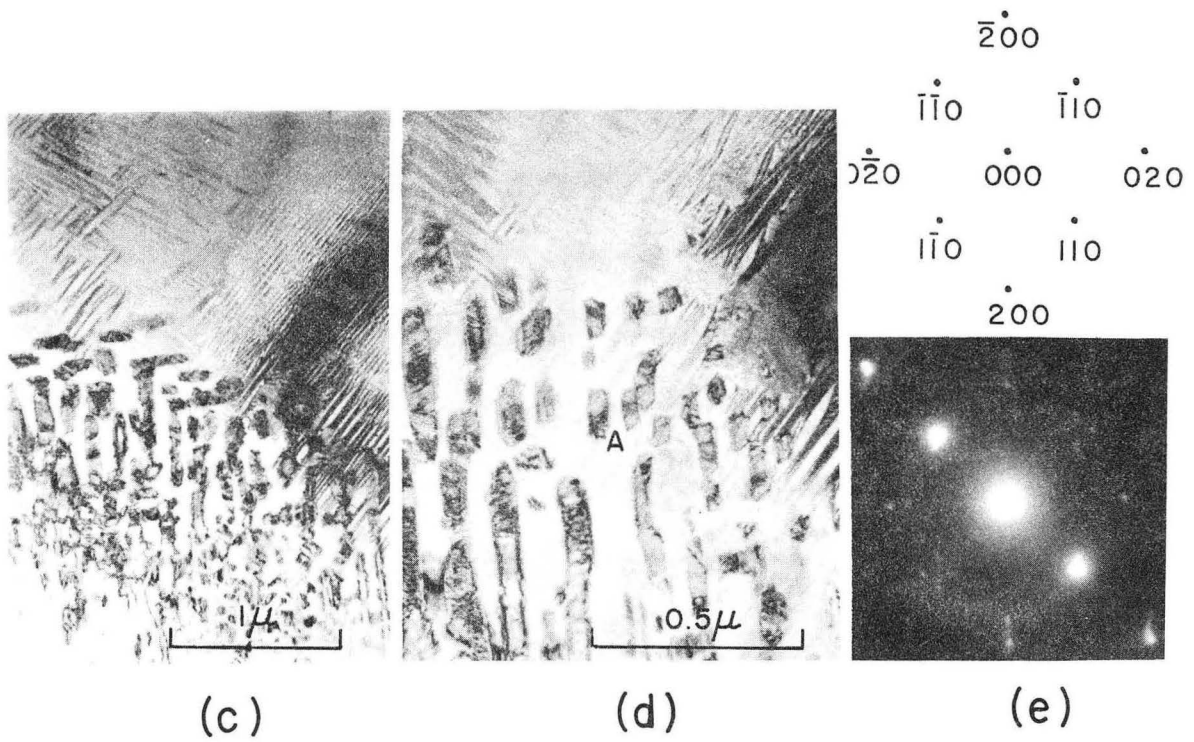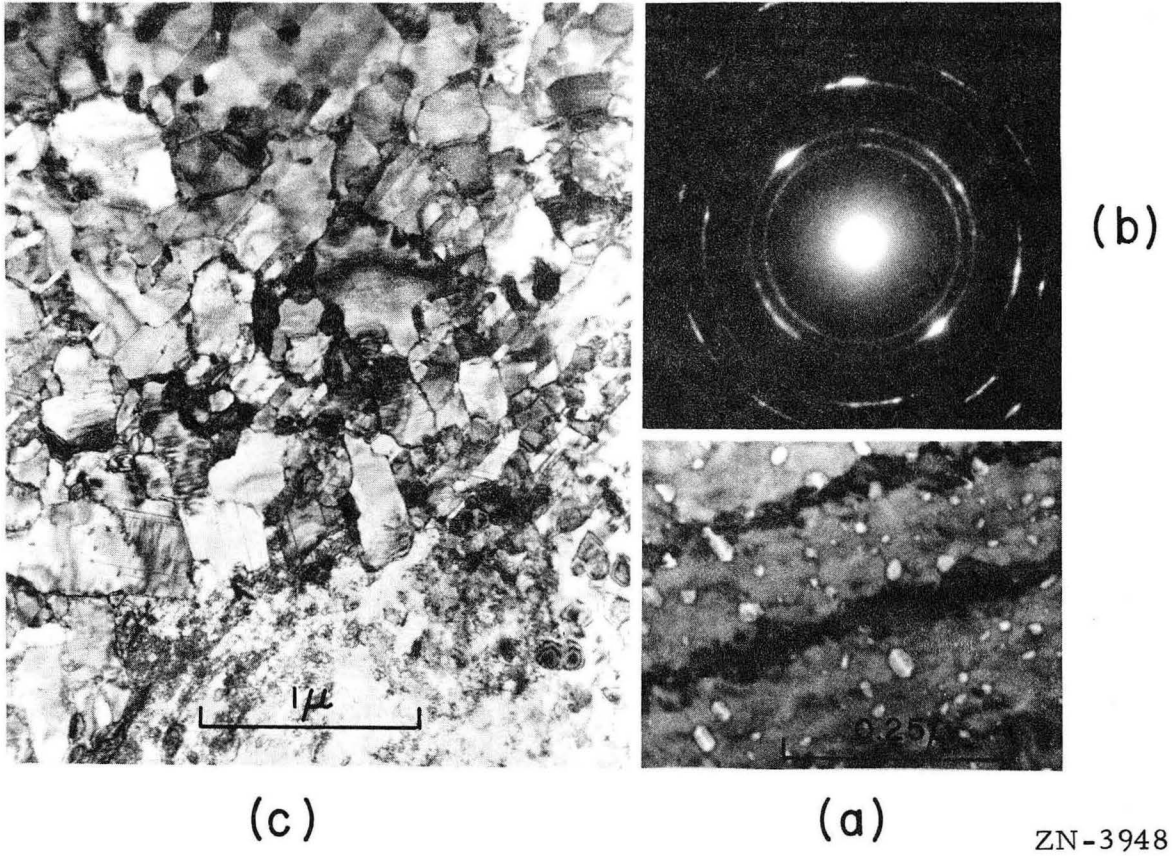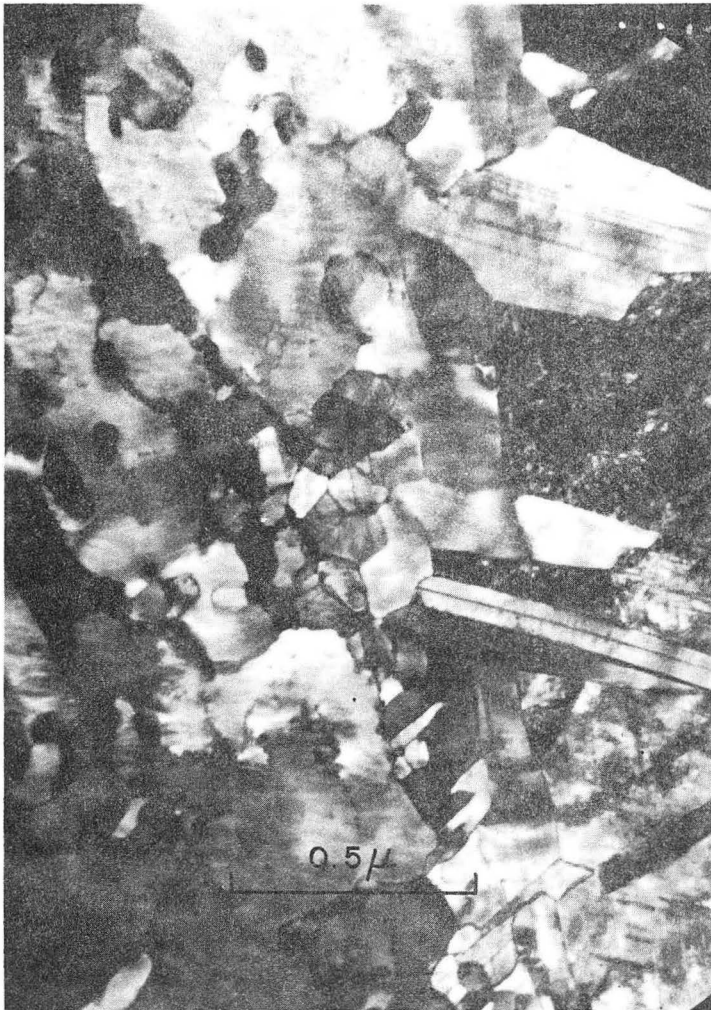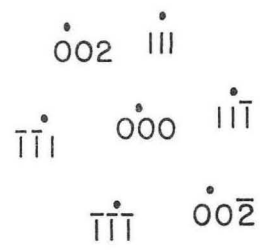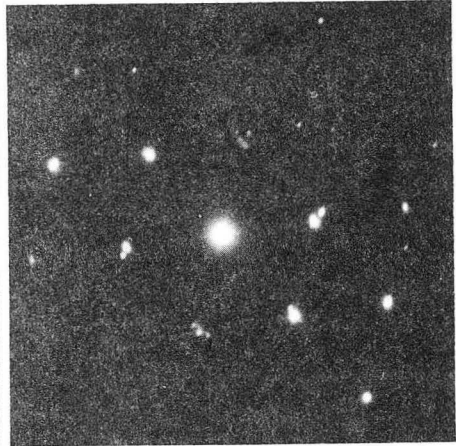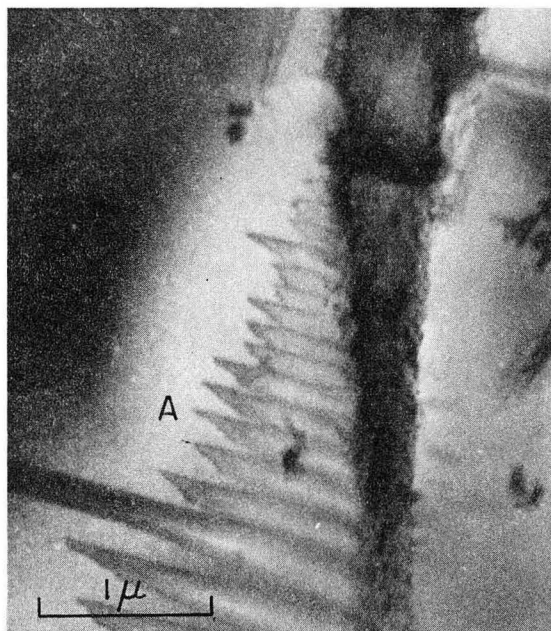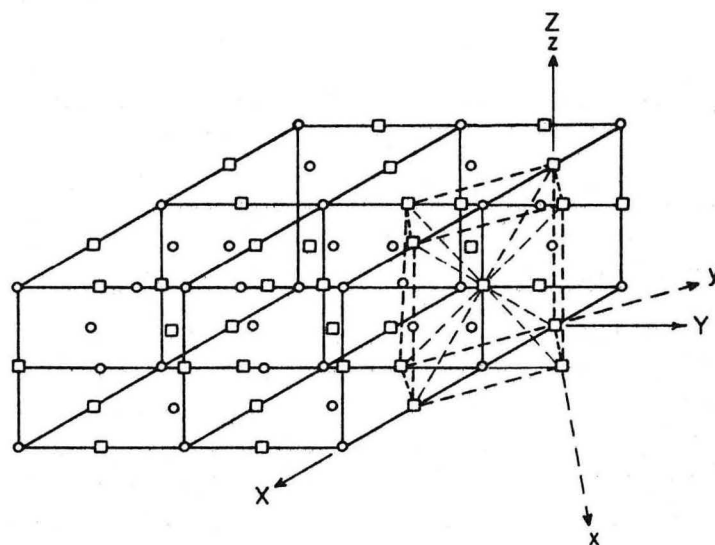
□ Nb ATOMS
○ OXYGEN ATOMS
X, Y and Z ARE COORDINATES IN NbO
x, y and z ARE COORDINATES IN Nb

MU-31914

Fig. 9.

(a)

(b)

MU-31915

Fig. 10.

Fig. 11.

Fig. 12.

MU-31917

(a)

(b)

$$0\overset{.}{1}1 \qquad \overset{.}{1}01$$

$$1\overset{.}{1}0 \qquad \overset{.}{0}00 \qquad \overset{.}{1}10$$

$$10\overset{.}{1} \qquad 0\overset{'}{1}\overset{.}{1}$$

ZN-3949

Fig. 13.